IOP Conf. Series: Journal of Physics: Conf. Series **882** (2017) 012004 doi:10.1088/1742-6596/882/1/012004

Advanced Imaging Techniques for Multiphase Flows Analysis

A. Amoresano, G. Langella, M. Di Santo, P. Iodice
University of Naples "Federico II" - Via Claudio 21 80125 Naples

amedeo.amoresano@unina.it

Abstract. Advanced numerical techniques, such as fuzzy logic and neural networks have been applied in this work to digital images acquired on two applications, a centrifugal pump and a stationary spray in order to define, in a stochastic way, the gas-liquid interface evolution. Starting from the numeric matrix representing the image it is possible to characterize geometrical parameters and the time evolution of the jet. The algorithm used works with the fuzzy logic concept to binarize the chromatist of the pixels, depending them, by using the difference of the light scattering for the gas and the liquid phase.. Starting from a primary fixed threshold, the applied technique, can select the 'gas' pixel from the 'liquid' pixel and so it is possible define the first most probably boundary lines of the spray. Acquiring continuously the images, fixing a frame rate, a most fine threshold can be select and, at the limit, the most probably geometrical parameters of the jet can be detected.

1. Introduction

The study of the phenomena of two phase systems is an important topic in the academic research [1]. It regards a lot of application in several fields like Mechanical Industry, Biology [3], Chemical [4] Aerospace [5] etc…The development of objective detection criteria for multiphase flow regimes has been the central research subject among many researchers during the recent past. One of the first research works on this subject is the one by Hubbard and Dukler (1966) [6] in which different flow regimes were characterized through their spectral signatures of temporal pressure signals. An interesting short review of the technique to analyses the dynamic of a two phase system by using imaging technique has been reported by has been done by F. L. Kleine et. Al in the introduction of their paper. [7]Many are the approaches used to analyses how two systems of different phase interact each other. In the last 10 years, with the coming of new sensors, the investigation of the two phase phenomena by images has grown considerably. The acquisition of data by using images technique has be done more carefully, because the acquired image couldn't represent the expected results. The acquisition can be affect by several mistake and uncertain depending on several other parameters. It is possible to sentence that digital images are subject to a wide variety of distortions during acquisition, processing, compression, storage, transmission and reproduction, any of which may result in a degradation of visual quality [8]. The quality image affect strongly the experimental results expected in special way if the measurements need several devices lying between the lens and the measuring region and if it the aim is to define the boundary lines between two or more phases. In this case can be useful to work with particular system that increase the contrast between the two fluids. For example the determination of the individual droplet diameter during the intake and the compression strokes was based on the intensity of the light scattered from the droplet which was subjected to the monochromatic irradiation of He-Ne laser with uniform intensity profile [9][10].

The determination of the boundary layers able to define the correct limit between the gas and the liquid phase can be complex and couldn't give the correct information especially if the interested phenomena developing themselves in very short time[11]. Due to all the cited parameters the correct pattern or other types of information extractable from the images can be treated with more sophisticated technique like statistical approach [12] and by using the wavelet transform to locate sub images with details coefficient able to define important particulars not always visible [13]. The data extracted from the recorded images hold several information can be used in different way. In this paper the data are considered like solutions of the Lagrangian equations [14] and define the work points of the dynamic system considered, i.e. the diagram of the phases. Because of the data representing the phenomena are images, their extraction have to be taken from them carefully. In other words the images and, consequently the associated matrix, can be treated with algorithms able to extract the wanted parameters. In this paper different measurements are presented like a two phase flow in a centrifugal pump where, by applying fuzzy method, bubbles, cluster of bubble and their trajectories have been calculated [15]. Measurements in a stationary spray where the lagrangian variable characterizing the spray is the half cone angle obtained from the images applying the Big Data approach [16].

2. Experimental set up

Two experimental different setup one for each experiment are presented. All the three cases use the same camera to record the images.

2.1. Centrifugal pump setup

Experimental analysis that follows numerical calculations has pointed out two-phase flow behavior by means of optical techniques. In Figure 1 a schematic layout experimental system has shown of the. A CCD image acquisition device has been used with high rate of frame per second. In order to visualize the two phase flow rate, the aspiration duct and the external flange of the impeller are transparent (fig 2). In this way it is possible to observe the behavior of the two phase flow outside and inside the impeller. The flow is visualized in the transparent duct (Fig.2) to study the flow field characteristics in the stationary case to understand the distribution of the gas phase inside the impeller. For the recording of the frames, a high speed CCD camera is used. The dissipation phenomena are quantified by the electrical balanced motor. The amplitude of the rotation around the zero value of the rotation axis is strongly related with the quantitative presence and permanence of the gas phase inside the impeller

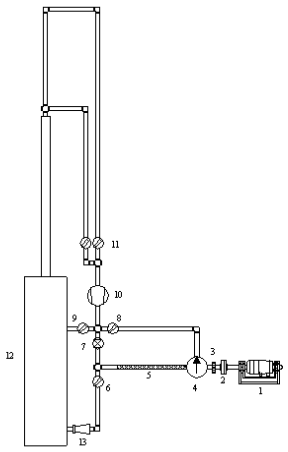

1 Triphase electrical balance motor
2 Double Hooke's joint
3 Magnetic Pick - up
4Centrifugal pump
5 Transparent Duct
6 Ball valve
7 By - Pass Valve
8 Lamination valve
9 Ball valve
10 Aero meter
11 Ball valve
12 water tank
13 water flowrate

Figure 1. Layout of the experimental setup

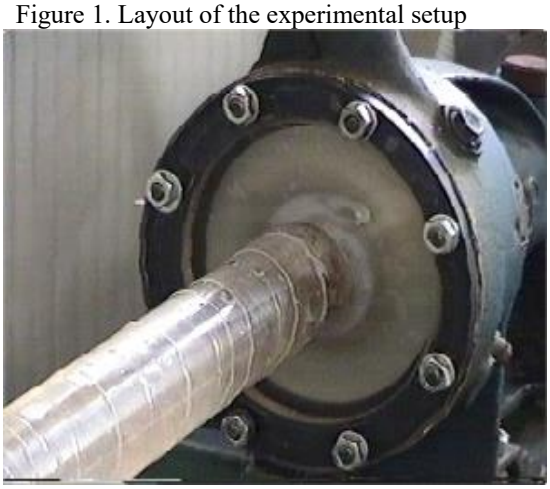

Figure 2 Pump working with two phase flow. Particular of the transparent flange

2.2. A Stationary spray experimental setup

The atomizer is set up on a vertical test (Fig.3) stand which allows the atomizer to translate both in vertical and in horizontal directions with steps of 1 mm, allowing to measure at different points in the vertical plane. A laser source (λ = 514.5 nm) generates a laser line that becomes a laser beam due to a divergent lens intercepting the spray to a centerline of his projection on the axial plane [17]. The laser sheet intercepts the spray exactly in the centerline and produces a planar image of the spray like shown in fig 4.

The laser beam induces the light scattering phenomenon when in contact with the liquid and the formed image (Fig. 4) can be acquired by using an optical device. In this case has been used a fastcam Photron Fastcam PCI. It is placed with its optical axis with an angle of 90° with respect to the laser sheet. The image sequences are recorded and stored in raw or bitmap format to acquire all the information.

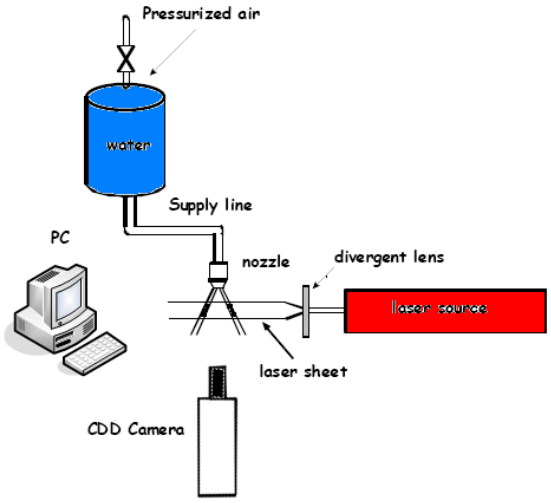

Figure 3- Experimental setup of data acquisition of stationary spray

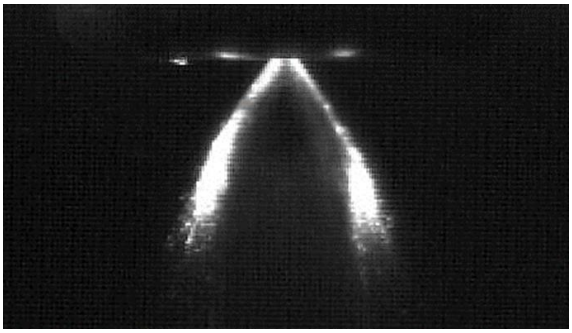

Figure 4- Planar image generated by a laser beam with a hollow cone spray

3. Data processing by fuzzy logic approach

In this paper, we had neither target images nor information about the final result of segmentation and classification, so we went towards the realization of a Multilayer Perceptron (MLP) not supervised but self-organized. Such multilayer is structurally and functionally different from a traditional MLP. Unlike supervised learning networks [18-21], in which the operator selects the examples for the training by assigning both the input arrays and output ones, the not supervised learning networks receive only arrays in the input stage. The final configuration of the weights of individual neurons allows to subdivide the elements supplied to the input into "similarity" groups which represent a classification. The Self Organizing Maps, therefore, can be considered as classifiers whose classes are arranged on a two-dimensional grid. Thanks to this pattern the Self-Organizing Maps keeps the topology of the input space. This means that if two inputs are neighbors, they are grouped in the same class or in closer classes on the two-dimensional grid. Then, the map tries to represent all the available observations by using a restricted set of arrays. Such arrays are ordered on a two-dimensional grid in such a way that similar arrays are disposed closer to each other while, conversely, the different ones are disposed far from each other. The greater is the difference larger will result the distance on the map.

The node output of a level (Fig. 5) is transmitted to the nodes of another layer by “links” which can amplify or attenuate or suppress these outputs through "weighted factors." Except for the nodes belonging to the first layer (input), the overall input to each node is the sum of the weighted outputs of nodes belonging to the previous level.

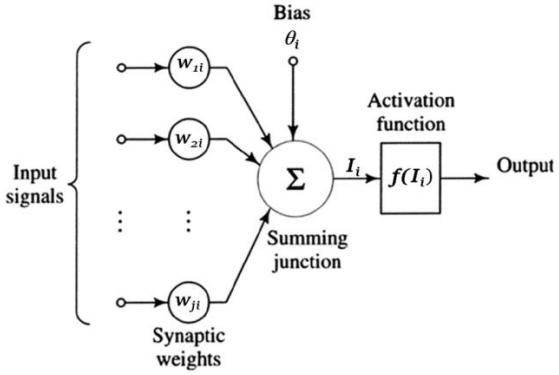

Figure 5. Information flow through the i[th] network node.

Each node is activated depending on input and activation function related to the node itself.

Each node is enabled depending on the input and on the activation function of node itself. The total input (I_i) to the i^{th} unit (node) of each layer is given by

$$I_i = \sum_j w_{ij} o_j \quad (1)$$

o_j being the output of the j^{th} neuron of the previous layer and w_{ij} the connection, weighed between the i^{th} node of a layer and the j^{th} one of previous layer.
Each node output is evaluated as:

$$o_j = f(I_i) \quad (2)$$

wheref is the activation function, sigmoidal in our case:

$$f(x) = \frac{1}{1 + e^{-(x-\theta)/\theta_0}} \quad (3)$$

Using the sigmoidal function to calculate the output of a network rather than a step function allows the classification of complex objects rather than divide the input pattern with simple lines.

3.1. Network structure

A three layers network was developed in the present work (Fig. 6). Each level (*layer*) is made of MxN neurons (MxN imagine). Each neuron corresponds to a single pixel. Between the input and the output layer there must be a number of layers greater than zero. Neurons belonging to a same layer do not have connections between each other. Each neuron of a layer is connected to the corresponding neuron of the previous layer as well as to the neurons belonging to the chosen neighborhood (N^d). In this way, each neuron on the layer *i* (*i >1*) will have $|N^d| + 1$ (dove $|N^d|$ is the number of pixels in N^d) links of the *(i - 1)*th layer.
For the case N^1 a neuron has 5 links, while for the N^2 it has 9 links, and so on. For border nodes the number of links may be less than $|N^d| + 1$. Each neuron belonging to the output layer is also connected to the corresponding neuron on the input layer.

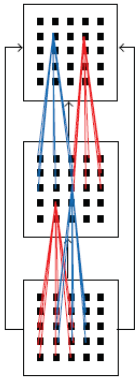

Figure 6. Scheme of a self-organizing multilayer neural network.

The proposed structure differs from a traditional *MLP* by the following points:

- link distribution;
- connection (feedback) from output layer to the input one.

3.2. Learning

The guiding principle allowing the network to learn is to let the network itself to learn from its mistakes. The input to a neuron belonging to the input layer is a real number in the interval [0,1] proportional to the value of the gray level of the corresponding pixel. Since the interest was in the elimination of noise and in the extraction of spatially compact regions, all weights were initially set

equal to 1. No external bias is imposed on weights. In this case random assignment of the weights could act as a pseudo - noise, altering accordingly the compactness of the regions extracted. Since all weights are set equal to 1, initially the total input for each node lives in $[0,n_e]$ where n_e is the number of links of each neuron. From here, we can also set the threshold value of θ (transport function for input / output eq. (3)) by

$$\theta = \frac{n_e}{2} \tag{4}$$

half total of the input rang

The input value I_i for each neuron of the i^{th} layer (except the input layer) is calculated by Eq. (1). The state of the neurons in this layer is calculated through the transport function *f (x)*, eq. (3). These outputs are used as inputs to the next layer. The image is provided by MxN pixels; each pixel has a value in the range [0,1]. Hence the fuzzy aspect of the problem: each pixel is an element of the fuzzy-set more or less clear or more or less dark. The support of this fuzzy-set is equal to the number of neurons of the output.

The degree of blur (fuzziness) of this set, as a whole, can be considered the error as well as the instability of the whole system since this will reflect the deviation from the "state" of the network desired. In this way there are not target a-priori as output values. We can take the blur value to measure the error of the system and back- propagate it in order to "tune" the weights, reducing it with time (epochs), at least down to zero. Therefore, the measure of the error E, can be adopted as a function capable of measuring the degree of blur, that is to say

$$E = g(I) \tag{5}$$

where *I* is the blur level of the fuzzy set (index of fuzziness).

After adopting the weights, the output of the neurons belonging to the output layer is "passed" to the corresponding neurons of the input layer. The second step goes on taking these as input. The iteration (update of weights) is continuous until the entire system stabilizes, that is to say that the error (measure of blur) becomes small. In this situation most of the neurons belonging to the output layer will assume the values “0” or “1”. Therefore, neurons with output value “0” will constitute a group while those having “1” will constitute another one. In this way the final image should present only compact regions in well-defined edges. In the cases where there is a no a-priori knowledge of the image (clustering problems) such a system is very instable.

In the case of a fuzzy set, we know that the index of indeterminacy (or blur) is minimum when the membership value of all the elements is “0” or “1” and is maximum when all the values are 0.5. Consequently, a neural network is stabilized when all the values of the output layer are “0” or “1” and is maximum (network unstable) when all values are equal to 0.5.

4. Results

The first step to have a good response applying the technique above described is to record a large number of frames. In this way the fuzzy logic and the related statistical approach give results strongly reliable. It want to emphasize that the found contour between gas and liquid phase are not the real contours but the most probably contours.

4.1. Centrifugal Pump

By using the CCD camera Photron Fastcam the sequence of the behaviour of air bubbles inside the impeller has been carried out. A typical sequence of the air bubbles behaviour has been rebuilt and it is shown in Fig.7

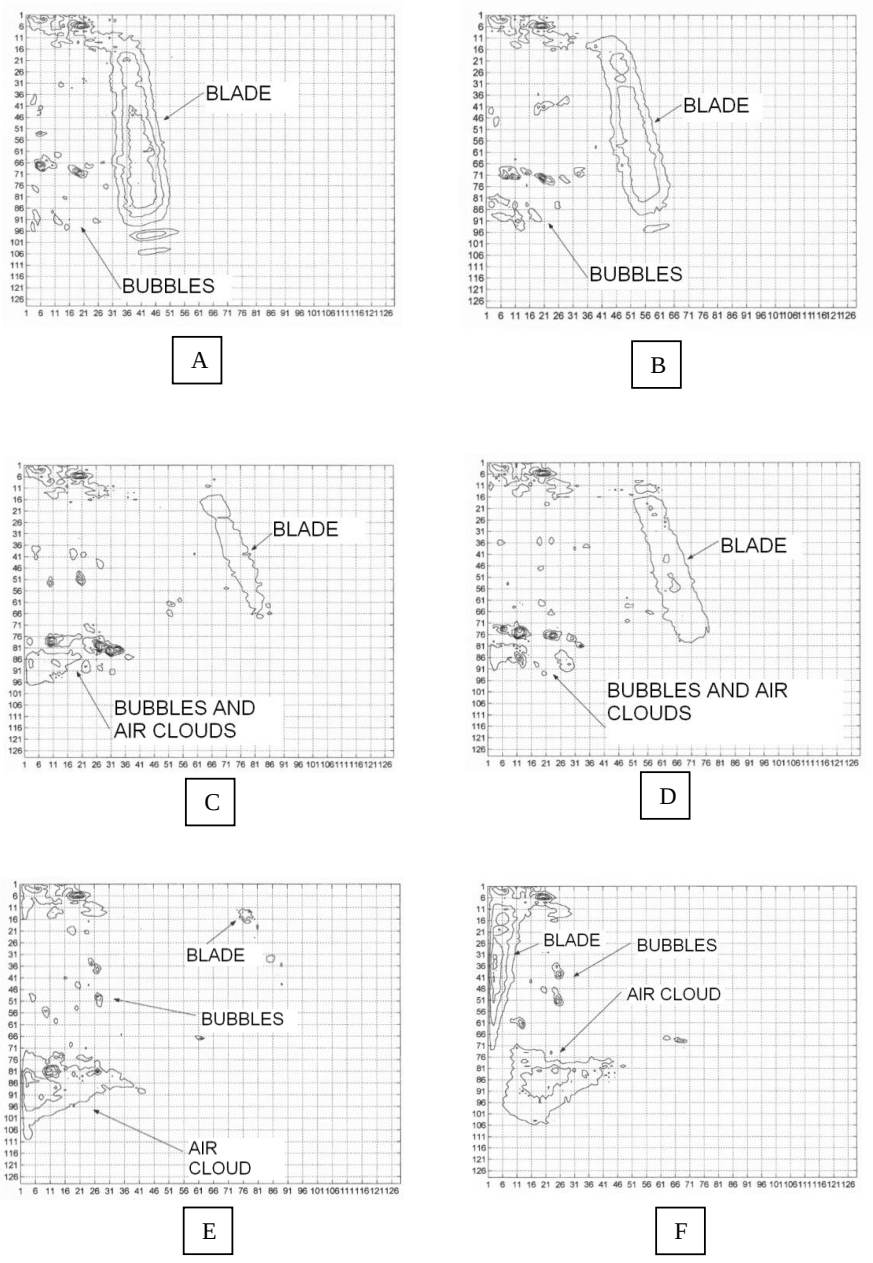

Fig. 7 a,b,c,d,e,f. Trajectory and behavior of air bubble inside a centrifugal pump

Particles that start from the low-pressure blade, or near this region, collide with the blade, slide on its surface, and go to the upper zone in the outlet zone of the rotor. The particles that crowd this region will change the blade profile and also the components of the velocity. Furthermore, experimental

analysis showed that air bubbles move inside the inlet duct on the upper side of the blade and crowd near the inlet flange. This is a very important wake point. In fact, if the air flow rate is relatively high in this region the bubbles can coalesce and for bubbles that the impeller is not able to break in to smaller sizes. It is well documented that bubbles with diameter in the range [0.1-0.2] mm pass easily from the inlet region to the outlet region following, with a good approximation, the water stream lines inside the impeller. Bubbles with $0.3 < d < 0.5$mm can detach from the coalescence region and move inside the blade to the blade duct from the high pressure region to low pressure region until the impact with the blade. These bubbles inside the impeller are governed by the balance of the pressure gradient, momentum, and drag force and can find the equilibrium point inside the impeller. Growing the range of diameter of the bubbles $0.6 < d < 0.8$–1mm, the equilibrium point moves to the eye of the pump and the bubbles can coalesce with the bubbles near the inlet flange. These conditions can also cause the total block of the water flow rate. By contour extraction software it is possible to evaluate the extension of the gas phase with respect to rotor vane, as reported in Figure 12.The cited sequence, from (a) to (f), has been acquired at 1 kHz and so the behavior of bubbles can be investigated duct by duct, from bubble motion to coalescence.

In Figure 7 (a), by contour analysis software, small bubbles starting from the inner radius, according to numerical results, move towards the blade side. In Figure 7(b) all bubbles coming from the rotor inlet, increasing radial coordinate, begin to coalesce, in small clusters. In figures. 7 (c), 9 (d), 9(e), and 9(f), coalescence goes on, generating a gas volume which keeps on invading the whole van. Energy transfer, due to Euler equation, is different between gas and liquid phases. If the coalescence phenomenon goes on, the percentage of gas will be more significant of the liquid phase and momentum variation transferred will be as small as liquid flow which rate decreases to zero. With such analysis a correlation between rotor angular speed, water flow rate, and gas phase extension can be carried out, identifying the limit of the work condition.

4.2. Stationary Spray

As demonstrated in previous research works [21], the single half-angle cone allows to characterize most of the spray. On the base of these results, and considering the difficulty to study both the “moustaches” Fig 4., due to the complexity of the whole system and process that would have led to incomparable values, we decided to analyze only the right spray side, which is the more fare from the laser source, focusing on the internal angle. In fact, the internal angle is much more interested by turbulence compared to the outer angle, due to the complex fluid-dynamics phenomena that take place around the atomizer axis both inside and outside, which lead to irregularities on the internal spray contours, as shown in fig.10. These irregularities influence a lot the spray evolution and need to be understood more. Therefore, to better catch the effective value of the angle, avoiding these irregularities, the AOI (Area of Interest) has been focused only on the first about two millimeter just outside the atomizer instead of the whole illuminated spray area.

The half-cone angle has been defined as the one formed by the spray axis and the segment between the hypothetical nozzle exit, considered as a point, and the middle point of the best fit curve that linearizes the most likely internal spray edge, as shown in Fig.11. The axis can be considered perfectly vertical and central in the image if the system is well regulated. The analysis of the image foresees to individuate the position of the points that belong to the most likely internal spray edge, defining an algorithm based on the brightness gradient, which is related to the grey value of the 8 bit image. As is well known, Matlab assigns to each image a (i,j) pixel matrix, where i is the row index and j the column one. These values depend on the image brightness ranging from 0 to 255; the lowest ones are dark pixels, while the highest are light pixels.

The image has elaborated by using neural network previous described, pixels outside the spray contours are usually black, then dividing the image in two equal parts at the nozzle axis, considering the right side only, where is visualized the right spray “moustache”, and choosing a low gradient threshold (about 5 points between the j pixel and j+1 one) it is possible, for each row, starting from the

first column j=1, to individuate every pixel that meet the threshold criteria. The first of these is the pixel which most likely correspond to the internal edge, while the last one most likely correspond to the outer edge instead, as shown in Fig. 10.

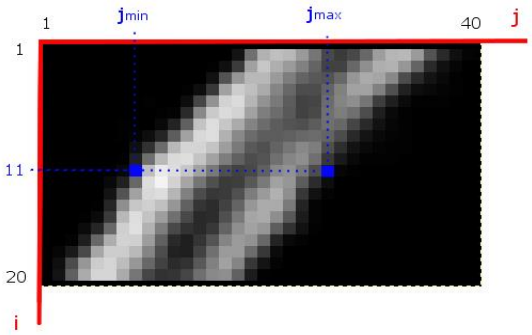

Fig. 10 Boundary region of the spray

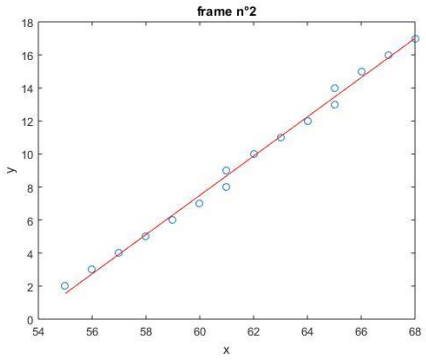

Fig.11 Best fit curve of the frame n°2

Starting from the elaborated images it is possible to calculate with a good confidence the half angle, or better the alfa angles of each fuzzy image and to define its variation band as reported in Fig. 12

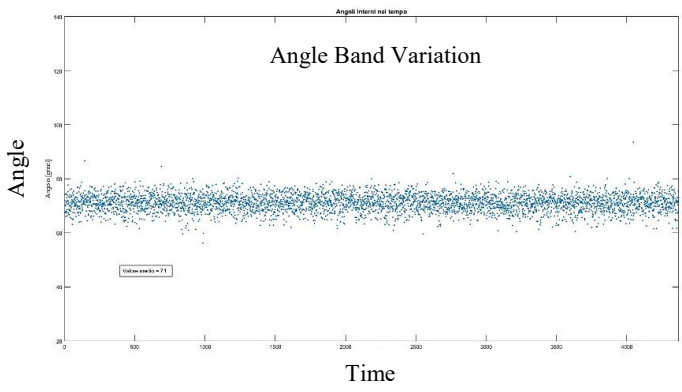

Fig.12 Angle band variation

4. Conclusion

In this paper the methodology to obtain information about a two phase fluid have been discussed. Have been presented two experiments, one related to the air bubbles moving inside an impeller pumping water and the second related to a stationary spray atomizing a liquid fluid. Both the experiments have been analysed by using the images to define their characteristics. To define better for the first the bubble's trajectory and for the spray a characteristic parameter like the half cone angle measures in the first 14mm starting for the tip an innovative approach, based on the use of a Fuzzy Logic coupled to a Neural Network, has been applied for describing their fluid dynamic and morphological behaviour..

The Fuzzy Logic coupled to a Neural Network allowed to objectively define both the interface (boundary layer) of the gas liquid interface and of the liquid-gas jet as a function of a threshold function. This approach, based on analysis of quasi- statistical data (Fuzzy Logic, Multivariate analysis, neural networks), is designed to extract more information from the images obtained from the high definition camera. In fact, assumed that digital images are two-dimensional arrays acquired over time, they define a 3D matrix and therefore it is possible to characterize the space-time evolution of areas at high-density present in liquid.

The digital image processing through the Neuro - Fuzzy Network opens up research on fuel injection systems to new scenarios. A careful investigation of the threshold values to be used in the neural network will lead to the realization of binarized images where you can also distinguish the finely atomized zone from the evaporated one and to well define the boundary layer between gas and liquid phase. In this way it can be a valuable diagnostic tool useful to understand in the centrifugal pump the vacuum fraction and the energy loss pumping a two phase fluid and in a stationary spray how maximize the efficiency of combustion.

References

[1] R. A. S. Brown, G. W. Govier "High-speed photography in the study of two-phase flow" The Canadian Journal of Chemical Engineering Volume 39, Issue 4 August 1961 Pages 159–164

[2] Dongwhi Choi, Donghyeon Lee & Dong Sung Ki "A Simple Approach to Characterize Gas-Aqueous Liquid Two-phase Flow Configuration Based on Discrete Solid-Liquid Contact Electrification" Scientific Reports 5, Article number: 15172 (2015) doi:10.1038/srep15172

[3] Armen R. Kherlopian, Ting Song, Qi Duan, Mathew A. Neimark, Ming J. Po, John K. Gohagan and Andrew F. Laine, "A review of imaging techniques for systems biology" BMC Systems Biology20082:74 DOI: 10.1186/1752-0509-2-74

[4] S. Anweiler, M. Masiukiewicz "Application Of Stereology For Two-Phase Flow Structure Validation In Fluidized Bed Reactors" Thermal Science: Year 2016, Vol. 20, No. 4, pp. 1199-1208

[5] A. Lecuona, P. A. Sosa, P. A. Rodríguez and R. I. Zequeira "Volumetric characterization of dispersed two-phase flows by digital image analysis" Measurement Science and Technology, Volume 11, Number 8

[6] Hubbard, M. G. and Dukler, A. E., 1966, "The Chacacterization of Flow Regimes for Horizontal Two-Phase Flow", Proc. Heat Transfer and Fluid Mech, Eds. M. A. Saad and J. A. Moller, Stanford University Press.

[7] J. Braz. Soc. Mech." Time-frequency analysis of intermittent two-phase flows in horizontal piping"

Journal of the Brazilian Society of Mechanical Sciences and Engineering vol.26 no.2 Rio de Janeiro Apr./June 2004

[8] Zhou Wang, Alan Conrad Bovik, Hamid Rahim Sheikh, Eero P. Simoncelli, "Image Quality Assessment: From Error Visibility to Structural Similarity" Ieee Transactions On Image Processing, Vol. 13, No. 4, April 2004

[9] Kadota, T., Mizutani, S., Wu, C., and Hoshino, M., "Fuel Droplet Size Measurements in the Combustion Chamber of a Motored SI Engine via Laser Mie Scattering," SAE Technical Paper 900477, 1990, doi:10.4271/900477.

[10] Montanaro, A., and Allocca, L., "Flash Boiling Evidences of a Multi-Hole GDI Spray under Engine Conditions by Mie-Scattering Measurements", SAE F&L Congress, Kyoto 2015, JSAE 20159062, SAE 2015-01-1945

[11] Chacon-Murguia, M.I., and Ramirez-Alonso, G. "Visual, Fuzzy-neural Self-adapting Background Modeling with Automatic Motion Analysis for Dynamic Object Detection", Applied Soft Computing 36 (2015) 570–577

Sekoguchi, K., Inoue, K. and Imasaka, T., 1987, "Void Signal Analysis and Gas-Liquid Two-Phase Flow Regime Determination by a Statistical Pattern Recognition Method", JSME International Journal, Vol. 30, No. 266, pp.1266-1273.

[12] C. Sunde, S. Avdic, I. Pafzsit. "Classification Of Two-Phase Flow Regimes Via Image Analysis And A Neuro-Wavelet Approach" Progress in Nuclear Energy, Vol. 46, No. 3-4, pp. 348-358, 2005

Melbourne, I., and Nicol, M., "Statistical properties of endomorphisms and compact group extensions", Preprint, Un. of Surrey, UK, 2003.

[13] Amoresano, A., Langella, G., Niola, V., and Quaremba, G., "Advanced Images Analysis of Two Phase Flow Inside a Centrifugal Pump", Advances in Mechanical Engineering, Volume 2014, Article ID 958320, 11 pages http://dx.doi.org/10.1155/2014/958320

[14] Allocca, L., Montanaro, A., Amoresano, A., Langella, G., Niola, V., Quaremba, G., "Chaos Theory Approach as Advanced Technique for GDI Spray Analysis" SAE Technical Paper 2017-01-0839

[15] T Marchione, C Allouis, A Amoresano, F Beretta "Experimental investigation of a pressure swirl atomizer spray" Journal of Propulsion and Power 23 (5), 1096-1101

[16] Montanaro, A., and Allocca, L., "Flash Boiling Evidences of a Multi-Hole GDI Spray under Engine Conditions by Mie-Scattering Measurements", SAE F&L Congress, Kyoto 2015, JSAE 20159062, SAE 2015-01-1945

[17] Castelli I., Trentin E. "Combination of Supervised and Unsupervised Learning for Training the Activation Functions of Neural Networks", Pattern Recognition Letters 37 (2014) 178–191

[18] Tsoukalas L.H., Uhrig R.E., "Fuzzy and Neural Approaches in Engineering. John Wiley & Sons Inc.", NY, USA (1997)

[19] Iosifidis A., "Extreme Learning Machine Based Supervised Subspace Learning", Neurocomputing 167 (2015) 158–164

[20] Wasserman P.D., "Advanced Methods in Neural Computing", Van Nostrand Reinhold, NY (1993)

[21] A Amoresano, G Langella, V Niola, G Quaremba "A Statistical Method to Identify the Main Parameters Characterizing a Pressure Swirl Spray" International Review of Mechanical Engineering (IREME) 7 (6), 1007-1013